Journal of Physics: Conference Series **88** (2007) 012051 doi:10.1088/1742-6596/88/1/012051

Convergent close coupling calculations of two-photon double ionization of He

A. S. Kheifets[♯], I. A. Ivanov[♯] and Igor Bray[♭]

[♯]Research School of Physical Sciences, The Australian National University, Canberra ACT 0200, Australia

[♭]ARC Central for Matter-Antimatter Studies, Curtin University, GPO Box U1987, Perth, WA 6845, Australia

E-mail: A.Kheifets@anu.edu.au

Abstract. We review recent applications of the convergent close-coupling (CCC) method to studies of two-photon double ionization (TPDI) of He. In a weak-field regime, the electron-photon interaction can be treated within the lowest order perturbation theory (LOPT) whereas the electron-electron interaction is included in full. The intermediate states of the target can either be represented by a discrete set of B-splines in a box or summed over with an average weight (closure approximation). In a non-perturbative regime, we solve the time-dependent Schrödinger equation on a square-integrable basis and project this solution on a set of CCC final states. In both regimes, we are able to calculate reliably the total integrated and fully differential TPDI cross-sections.

Besides purely numerical results, we introduce a convenient analytical parametrization of the TPDI amplitude in the manner similar to single photon double ionization. Aided with this parametrization, we observe two distinctly different modes of correlated motion of the photoelectron pair. We also derive the angular anisotropy parameters and the recoil ion momentum distribution for TPDI of He. The latter can be compared with recent experimental observations.

1. Introduction

Convergent close-coupling (CCC) method has been a very successful tool for theoretical studies of single-photon double ionization (SPDI) of He and other two-electron atomic and molecular targets [1]. To apply the CCC technique to the two-photon double ionization (TPDI) problem, a further development of the method is needed. Firstly, integration over all the intermediate states of the target is required. This involves evaluation of the ill-defined continuum-continuum dipole matrix elements. To circumvent this difficulty, we perform our calculations in the Kramers-Henneberger gauge of the electromagnetic interaction [2]. As an alternative and much less time consuming method, we use the closure approximation to carry out summation over all the intermediate target states. As the result of this procedure, we end up with evaluation of the monopole and quadrupole matrix elements between the correlated ground state and the CCC final state. This procedure was developed in an earlier work on the second Born treatment of the electron impact ionization-excitation and double ionization of He [3].

Secondly, in contrast to the weak-field SPDI, the theoretical description of TPDI at large field strengths requires stepping out beyond the perturbation theory formalism. This can be

achieved by numerical solution of the time-dependent Schrödinger equation (TDSE) on a square-integrable basis and subsequent projection of this solution on a set of CCC field-free states [4].

This Progress Report is organized as follows. In Sections 2.1 and 2.2 we present our perturbative formalism relying on the closure approximation and utilizing the discrete set of B-splines, respectively. In Section 2.3 we describe our non-perturbative formalism based on the solution of the time-dependent Schrödinger equation on a square-integrable basis. In Sections 3.1-3.5 we present results for the total integrated and triply-differential cross-sections (TICS and TDCS), the symmetrized ionization amplitudes angular anisotropy parameters and the recoil ion momentum distribution.

2. Formalism

2.1. LOPT in closure approximation

We use the following second order perturbation theory expression for the total integrated cross-sections (TICS) of TPDI :

$$\sigma(\omega) = C_2\omega^{\beta} \sum_{\epsilon_f>0}\sum_{m_f}\int d\Omega_k \Big| \sum_i \int d^3p \frac{\langle\Psi_f(\boldsymbol{k})|\ \boldsymbol{e}\cdot\boldsymbol{d}\ |\Psi_i(\boldsymbol{p})\rangle\langle\Psi_i(\boldsymbol{p})|\ \boldsymbol{e}\cdot\boldsymbol{d}\ |\Psi_0\rangle}{E_0+\omega-p^2/2-\epsilon_i+i\delta}\Big|^2 \qquad (1)$$

Here the two-photon ionization constant $C_2 = 8\pi^3 c^{-2} a_0^4 \tau = 2.505\times10^{-52}$ cm^2 s^{-1} [5]. The vector $\boldsymbol{e}$ represents the polarization of light. The dipole operator $\boldsymbol{d} = \boldsymbol{d}_1 + \boldsymbol{d}_2$ where $\boldsymbol{d}_\alpha = \boldsymbol{r}_\alpha$, $\boldsymbol{\nabla}_\alpha$ and $Z\boldsymbol{r}_\alpha/r_\alpha^3$ in the length, velocity and acceleration gauges, respectively, the nucleus charge $Z = 2$ for helium. The exponent β depends on the gauge of the electromagnetic interaction, $\beta = 2$ in the length gauge. A correlated ground state wave function Ψ_0 is represented by a multi-configuration Hartree-Fock expansion [6].

In the CCC formalism, we represent the two-electron state by a close-coupling expansion over the channel states each of which is composed of a target pseudo state f and a Coulomb wave $\boldsymbol{k}$:

$$\Psi_f(\boldsymbol{k}) = |\boldsymbol{k}f\rangle + \sum_j \sum\!\!\!\!\!\!\int d^3k' \frac{\langle \boldsymbol{k}f|T|j\boldsymbol{k}'\rangle}{E-k'^2/2-\varepsilon_j+i0}\ |\boldsymbol{k}'j\rangle\ . \qquad (2)$$

Here $\langle \boldsymbol{k}f|T|j\boldsymbol{k}'\rangle$ is half-on-shell T-matrix which is found by solving a set of coupled Lippmann-Schwinger equations [7]. The target pseudostates with positive energies $\epsilon_f > 0$ represent the doubly ionized final state. Implicit in Eq. (1) is the energy conservation $\epsilon_f + k^2/2 = 2\omega$. The CCC wave function representing two electrons in continuum can be obtained by projecting the positive energy pseudostate in Eq. (2) onto the Coulomb wave of matching energy:

$$\Psi(\boldsymbol{k}_1,\boldsymbol{k}_2) = \Psi_f(\boldsymbol{k}_1)\langle \boldsymbol{k}_2|f\rangle \quad , \quad \epsilon_f = k_2^2/2. \qquad (3)$$

If we assume that the integrand in Eq. (1) is a smooth function, we can take out an average energy denominator Δ and use the completeness of the CCC basis. This procedure, known as the closure approximation, will take us to the following result:

$$\sigma(\omega) = C_2\omega^{\beta}\Delta^{-2} \sum_{\epsilon_f>0}\sum_{m_f}\int d\Omega_k \Big|\langle\Psi_f(\boldsymbol{k})|(\boldsymbol{e}\cdot\boldsymbol{d})(\boldsymbol{e}\cdot\boldsymbol{d})\ |\Psi_0\rangle\Big|^2 \qquad (4)$$

The fully-resolved triply-differential cross-section (TDCS) can be written in the closure approximation as

$$\frac{d^3\sigma}{d\Omega_1 d\Omega_2\, dE_2} = C_2\omega^{\beta}\Delta^{-2}\Big|\langle\Psi_f(\boldsymbol{k}_1)|(\boldsymbol{e}\cdot\boldsymbol{d})(\boldsymbol{e}\cdot\boldsymbol{d})\ |\Psi_0\rangle\langle\boldsymbol{k}_2|f\rangle\Big|^2 \qquad (5)$$

2.2. LOPT with B-splines

To carry over summation over all intermediate states in Eq. (1), without relying on the closure approximation, we use the discretization method developed in Ref. [8] and applied to the problem of TPDI of helium in Ref. [9]. Within this procedure, the set of intermediate states in the PT expressions is replaced by the set obtained by diagonalization of the atomic Hamiltonian in a suitably chosen basis. Within this procedure, the second order amplitude entering (1) is calculated as:

$$\sum_{i\neq i_0} \left\langle \Psi_f(\boldsymbol{k}) \left| \hat{H}_{\rm int}^{\rm KH} \right| \Psi_i \right\rangle \left\langle \Psi_i \left| \hat{H}_{\rm int}^{\rm KH} \right| \Psi_0 \right\rangle (E_0+\omega-E_i)^{-1} - i\pi\rho^2 \left\langle \Psi_f(\boldsymbol{k}) \left| \hat{H}_{\rm int}^{\rm KH} \right| \Psi_{i_0} \right\rangle \left\langle \Psi_{i_0} \left| \hat{H}_{\rm int}^{\rm KH} \right| \Psi_0 \right\rangle ,$$

where Ψ_i is the discrete set of states, Ψ_{i_0} belongs to the energy shell $E_0 + \omega - E_{i_0} = 0$, $\rho^2 = 2(E_{i_0+1} - E_{i_0-1})^{-1}$.

To achieve accurate numerical results, it is necessary to ensure that the density of discrete states Ψ_i is sufficiently high near the position of the pole of the LOPT expansion. This can be achieved if we employ a basis composed of B-splines in a box and define a two-electron discrete states as $\Psi_i(\boldsymbol{r}_1, \boldsymbol{r}_2) = \sum_{n,m} C_i \; B_{nk}(r_1) B_{mk}(r_2) |l_1(1) l_2(2) L\rangle$. Here notation $|l_1(1) l_2(2)\; L\rangle$ is used for bipolar harmonics. The radial orbital $B_{nk}(r)$ is a basis spline of the order $k = 7$ with the knots located at the sequence of points lying in $[0, R_{\rm max}]$ where the size of the box $R_{\rm max}$ is varying between 30 a.u. and 70 a.u. Typical number of knot points was 40-45, they were distributed evenly in $[0, R_{\rm max}]$. The coefficients C_i in the B-spline expansion were obtained by diagonalizing the He atom Hamiltonian $\langle \Psi_i | \hat{H} | \Psi_j \rangle = E_i \delta_{ij}$. This diagonalization procedure in the subspace of the S-symmetry states q gave the ground state energy of $E_0 = -2.9004$ a.u.

2.3. Time-dependent formalism

When the field cannot be treated perturbatively, we rely on a direct numerical solution of the TDSE $i\,\partial\Psi/\partial t = \hat{H}\Psi$ for the helium atom in the presence of the external AC field. The atomic Hamiltonian $\hat{H} = \hat{H}_0 + \hat{V}_{12} + \hat{H}_{\rm int}(t)$ contains the non-interacting part $\hat{H}_0 = \boldsymbol{p}_1^2/2 + \boldsymbol{p}_2^2/2 - 2/r_1 - 2/r_2$, the Coulomb interaction $\hat{V}_{12} = |\boldsymbol{r}_1 - \boldsymbol{r}_2|^{-1}$ and the interaction with the external AC field $\hat{H}_{\rm int}(t) = f(t)(\boldsymbol{r}_1 + \boldsymbol{r}_2) \cdot \boldsymbol{F}_{\rm ac} \cos\omega t$. Here $f(t)$ is a smooth switching function which is chosen in such a way that it is zero for $t = 0$ and $t = 6T$, where $T = 2\pi/\omega$ is a period of the AC field. For $t \in (T, 5T)$ $f(t) = 1$, for $t \in (0, T)$ it grows monotonously, so that $f(t)$ and its derivative are continuous. Analogously, for $t \in (5T, 6T)$ $f(t)$ smoothly decays from 1 to zero. The total duration of the atom-field interaction is therefore $T_1 = 6T$.

The solution of the TDSE is sought in the form of expansion on a square-integrable basis

$$\Psi(\boldsymbol{r}_1, \boldsymbol{r}_2, t) = \sum_j a_j(t) f_j(\boldsymbol{r}_1, \boldsymbol{r}_2) \quad , \text{ where } \quad f_j(\boldsymbol{r}_1, \boldsymbol{r}_2) = \phi^N_{n_1 l_1}(r_1) \phi^N_{n_2 l_2}(r_2) \; |l_1(1) l_2(2)\; L\rangle \; . \quad (6)$$

The radial orbitals in Eq. (6) are pseudostates diagonalizing the He^+ Hamiltonian in a Laguerre basis: $\langle \phi^N_{nl} | \hat{H}_{\rm He^+} | \phi^N_{n'l'} \rangle = E_i \delta_{nn'} \delta_{ll'}$. Initial conditions for the solution of TDSE are determined by solving an eigenvalue problem using a subset of basis functions of the S-symmetry only. We integrate TDSE up to a time T_1 when the external field is switched off. Then we project the solution onto a field-free CCC wave function (3) representing two electrons in continuum. This prepares a set of the final states corresponding to various photoelectron energies E_1, E_2. Projection of the solution of the TDSE on the states of this grid geves us a probability distribution function $p(\boldsymbol{k}_1, \boldsymbol{k}_2)$ of finding the helium atom in a field-free two-electron continuum state $\boldsymbol{k}_1, \boldsymbol{k}_2$ at the time $t = T_1$. From this probability, we can compute TICS and TDCS:

$$\sigma(\omega) \;\; = \;\; \frac{C_2\,\omega^2}{W} \int p(\boldsymbol{k}_1, \boldsymbol{k}_2) \; d\hat{\boldsymbol{k}}_1 d\hat{\boldsymbol{k}}_2 dk_1 dk_2, \quad , \quad W = \int_0^{T_1} F_{\rm ac}^4(t) \; dt$$

$$\frac{d\sigma(\omega)}{dE_1 d\Omega_1 d\Omega_2} = \frac{C_2\,\omega^2}{W q_1 q_2\ \cos^2\alpha}\int p(\boldsymbol{k}_1, k_1\tan(\alpha)\ \hat{\boldsymbol{k}}_2)\ k_1 dk_1, \tag{7}$$

Momenta q_1, q_2 in Eq. (7) are defined on the energy shell: $E_1 = q_1^2/2$, $E - E_1 = q_2^2/2$, $\tan\alpha = q_2/q_1$, E is the excess energy.

3. Results

3.1. Total integrated cross-section

Results for the TICS of TPDI of He are presented in Figure 1. There are four different CCC calculations plotted in the Figure. The first set is the closure calculation using Eq. (4) in which the following estimate of the energy denominator Δ was used. We assumed that the main contribution to the sum over the intermediate states in Eq. (1) came from those terms where the energies of the intermediate electron $p^2/2$ was close to the energy of the final state electron $k^2/2$. Under this condition, the dipole matrix element between the intermediate and final continuum states in Eq. (1) will be strongly peaking. This condition leads to $\Delta \simeq \omega$. However, as is seen in Figure 1, this choice of the energy denominator gives the TICS which is far below other theoretical predictions [10–13]. Also, such a closure calculation gives the TICS which is flattening near the threshold of the sequential TPDI process. However, it was argued in Ref. [13] that the TICS should be increasing steeply near the threshold because of the growing contribution of the sequential process in which two atomic electrons are removed independently, one by one.

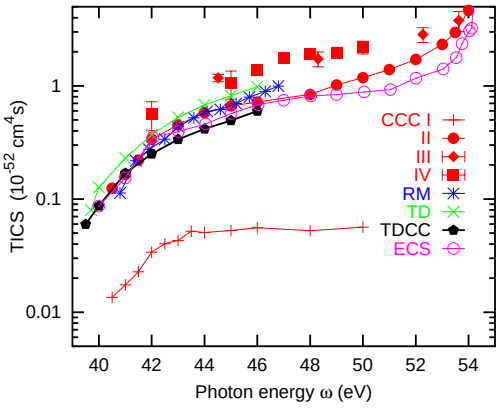

Figure 1. (Color online) The total integrated cross-section of the TPDI of He as a function of the photon energy. The four CCC calculations are shown: I - closure approximation, red plus signs; II - closure modified by sequential process, red circles; III - LOPT with B-splines, red diamonds; IV - TDSE, red squares. Calculations by other authors are as follows: R-matrix [10], blue asterisks; time-dependent (TD) basis [11], green crosses; time-dependent close-coupling (TDCC) [12], black pentagons; exterior complex scaling (ECS) [13], purple open circles.

Based on this argument, we reconsidered the choice of the energy denominator made in Ref. [14]. If we assume that the leading process is a sequential interaction of both atomic electrons with the field, the typical energy denominator should be of the order of $\Delta \simeq 0.5(\mathrm{IP}_{\mathrm{He}^+} - \mathrm{IP}_{\mathrm{He}})$ where $\mathrm{IP}_{\mathrm{He}}$ and $\mathrm{IP}_{\mathrm{He}^+}$ are the ionization potentials of the neutral He atom and the singly charged He^+ ion, respectively. In addition to this new choice of the energy denominator, we evaluated the matrix element of the lowest order sequential process explicitly taking it out from the closure sum. In this process, the two atomic electrons interact sequentially with the field but not with each other. It is this process that gives a steep rise of TICS near the sequential TPDI threshold. As can be seen from Figure 1, such a closure calculation modified by the sequential process is much closer to other literature results and demonstrates the correct behaviour near the sequential threshold.

In the same figure, we also show the TICS results obtained in the LOPT calculation with B-splines and the TDSE . These two sets of results are shown with error bars which indicate a typical accuracy of the corresponding method. The LOPT results are effected somewhat by the choice of the size of the box. The TDSE results may vary depending on the timing of the projection on the field-free continuum states (see Ref. [4] for detail). The LOPT and

TDSE results are very close. The latter calculation was performed for the field intensity of 3.5×10^{14} W/cm^2 corresponding to the electric field of the order of 0.1 a.u. Not surprisingly, both non-perturbative and LOPT results are close for such a weak field. However, it can be argued [15] that, for the field intensities as high as 10^{16} W/cm^2 in the XUV photon energy range, the ponderomotive energy of the electron is only 1% of the photon energy. This means that the higher order effects beyond two-photon absorption can be ignored and the use of LOPT is well justified.

3.2. Triply-differential cross-section

The fully-differential, with respect to the photoelectron energies and angles, TDCS can provide additional information on the mechanisms of two-electron escape and the role the many-electron correlations play in this process.

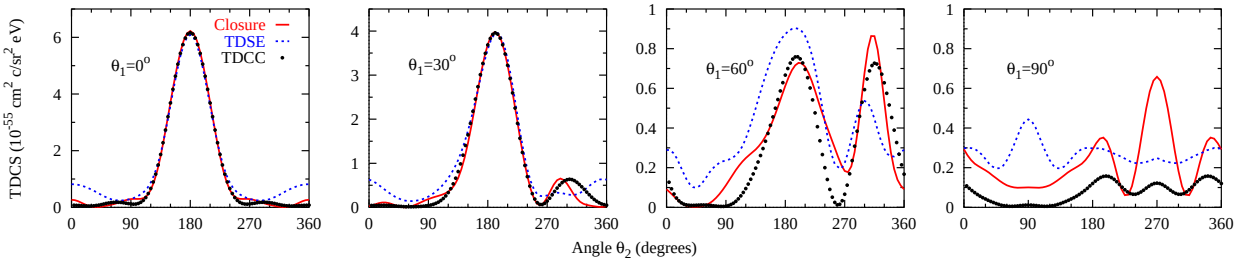

Figure 2. (Color online) TDCS of TPDI of He for the coplanar geometry at $\omega = 42$ eV, $E_1 = E_2 = 2.5$ eV and various fixed electron angles. The CCC calculation in the closure approximation from Ref. [14] (divided by 1.6) is shown by the red solid line. The TDSE calculation projected on the CCC final state from Ref. [4] (divided by 2.2) is shown by the blue dashed line. The black dots represent the TDCC results of Ref. [12].

In Figure 2 we show two CCC calculations (with closure and TDSE) of TDCS at $\omega = 42$ eV and equal energy sharing $E_1 = E_2 = 2.5$ eV in comparison with the TDCC result of Ref. [16]. Here the coplanar geometry is assumed in which the two photoelectrons are detected in the same plane with the polarization axis of linearly polarized light. One electron escapes at a fixed angle θ_1 and the second electron is detected on the full angular range. In the closure calculation, the CCC basis of the final state included $20 - l$ target states with orbital momentum l ranging from 0 to 6 (the so-called $20l6$ calculation). A more concise $15l3$ basis was used in a much more time consuming and computationally demanding CCC calculation with TDSE.

We see from Figure 2 that the closure CCC results are very similar, in shape, with the TDCC calculation of Ref. [16] in which the short field pulse interaction with the He atom was treated nonperturbatively. More thorough and extensive comparison of the two methods was made in Ref. [14] and confirmed this conclusion. Such a similarity can be interpreted in the following way. Due to the long range of the Coulomb force, the angular correlation pattern in the two-electron continuum is formed at large distances (and times) when the field pulse is long gone. It shows, therefore, little sensitivity to the details of the atom-field interaction which can be treated in the simplified closure approximation. The CCC results with TDSE shown in Figure 2 are also similar but exhibit more deviation from the TDCC calculation. This may be due to a smaller CCC basis size used in this particular calculation.

3.3. Symmetrized ionization amplitudes

The TDCS results of the previous section can be conveniently analyzed and interpreted by introduction of a simple parametrization in which the essential dynamic of the TPDI process

is separated from kinematic variables. Similar parametrization for SPDI process introduced in Ref. [17; 18] proved to be a very useful and convenient tool. In the most general way, the amplitude of the TPDI process can be present in the following form [19]:

$$F(\hat{\boldsymbol{k}}_1, \hat{\boldsymbol{k}}_2) = f_1(\hat{\boldsymbol{k}}_1 \cdot \boldsymbol{e})^2 + f_2(\hat{\boldsymbol{k}}_2 \cdot \boldsymbol{e})^2 + f_s(\hat{\boldsymbol{k}}_1 \cdot \boldsymbol{e})(\hat{\boldsymbol{k}}_2 \cdot \boldsymbol{e}) + f_0(\boldsymbol{e} \cdot \boldsymbol{e}) \tag{8}$$

Here the unit vectors $\hat{\boldsymbol{k}}_i = \boldsymbol{k}_i/k_i, i = 1, 2$ are directed along the photoelectron momenta and $\boldsymbol{e}$ is the polarization vector of light. Eq. (8) can be transformed to the Jacobian momenta $\boldsymbol{p} = \boldsymbol{k}_1 + \boldsymbol{k}_2$ and $\boldsymbol{q} = \boldsymbol{k}_1 - \boldsymbol{k}_2$ [20]

$$F(\boldsymbol{p}, \boldsymbol{k}) = f_p(\boldsymbol{p} \cdot \boldsymbol{e})^2 + f_k(\boldsymbol{k} \cdot \boldsymbol{e})^2 + f_{kp}(\boldsymbol{k} \cdot \boldsymbol{e})(\boldsymbol{p} \cdot \boldsymbol{e}) + f_0(\boldsymbol{e} \cdot \boldsymbol{e}) \tag{9}$$

In comparison, the SPDI amplitude has a much simpler structure: $D(\boldsymbol{p}, \boldsymbol{k}) = d_p(\boldsymbol{p} \cdot \boldsymbol{e}) + d_k(\boldsymbol{k} \cdot \boldsymbol{e})$. Under the equal energy condition $E_1 = E_2$, f_{kp} and d_k are vanishing and the SPDI amplitude $D(\boldsymbol{p}, \boldsymbol{k})$ depends on one vector $\boldsymbol{p}$ whereas $F(\boldsymbol{p}, \boldsymbol{k})$ retains dependence on both $\boldsymbol{p}$ and $\boldsymbol{k}$. The corresponding amplitudes f_p and f_k can be associated with the center-of-mass and relative motion, respectively. A gaussian ansatz $|f|^2 \propto a \exp\left[-4 \ln 2 (\pi - \theta_{12})^2 / \Delta\theta_{12}^2\right] + b$ can be applied to the squared amplitudes in which the width factor $\Delta\theta_{12}$ indicates the strength of the angular correlation in the two-electron continuum.

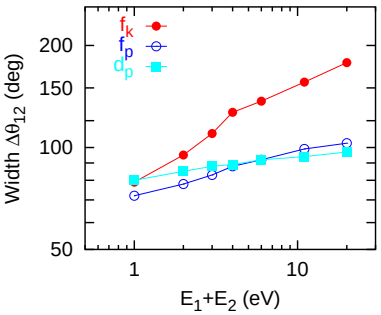

Figure 3. (Color online) The angular correlation width $\Delta\theta_{12}$ of the TPDI amplitudes f_p, f_k in comparison with the width of the SPDI amplitude d_p, all calculated at equal energy sharing $E_1 = E_2 = E/2$ and plotted versus the excess energy E. Center-of-mass motion: $F \propto f_p(\boldsymbol{p} \cdot \boldsymbol{e})^2$, $D \propto d_p(\boldsymbol{p} \cdot \boldsymbol{e})$. Relative motion: $F \propto f_k(\boldsymbol{k} \cdot \boldsymbol{e})^2$

The width factors, as functions of the excess energy $E = E_1 + E_2$, are plotted in Figure 3. We see a considerable difference between the the width factors of the amplitudes associated with the center-of-mass and relative motion. In the former case, large $\boldsymbol{p}$ favors $\boldsymbol{k}_1 \uparrow\uparrow \boldsymbol{k}_2$ which causes large Coulomb repulsion and hence a smaller Gaussian width. In the latter case, large $\boldsymbol{k}$ favors $\boldsymbol{k}_1 \uparrow\downarrow \boldsymbol{k}_2$ which is associated with a smal Coulomb repulsion and a larger Gaussian width.

3.4. Angular anisotropy parameters

By integrating Eq. (5) over $d\Omega_1$, we get the doubly differential cross-section (DDCS) which can be presented in the form

$$\frac{d^2\sigma}{d\Omega_2 dE_2} = \frac{d\sigma}{dE_2}\frac{1}{4\pi}\Big[1 + \beta_2 P_2(\cos\theta_2) + \beta_4 P_4(\cos\theta_2)\Big] \tag{10}$$

On the left panel of Figure 3 we show the β parameters in Eq. (10) for TPDI of He with linearly polarized light at the excess energy of 11 eV above the double ionization threshold which corresponds to the photon energy $\omega = 45$ eV. For comparison, on the right panel of the same figure, we show the β-parameter for SPDI at the excess energy of 20 eV (the photon energy $\omega = 99$ eV). The experimental data for SPDI are from Ref [21].

By comparing the left and right panels of Figure 1, we observe a significant qualitative difference between the β parameters for TPDI and SPDI. In the two-photon case, both β_2 and β_4 are large and positive. In contrast, in the single-photon case, the β_2 parameter varies widely from nearly zero for a very slow photoelectron to large positive values for a fast photoelectron.

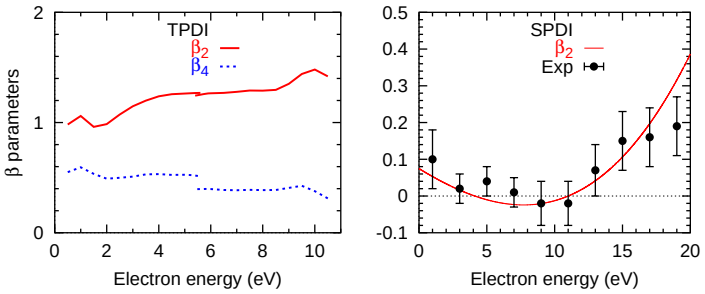

Figure 4. (Color online) Angular anisotropy β parameters for two-photon (left) and single-photon (right) double ionization of He at the excess energies of 11 and 20 eV, respectively. Experimental data for SPDI are from Ref. [21].

This energy dependence of β_2 can be interpreted as a gradual cross-over between two different regimes of SPDI. Nearly zero β_2 parameter of a slow photoelectron corresponds to a fully isotropic angular distribution which is a footprint of the shake-off mechanism. On the contrary, a large positive β_2 parameter for a fast photoelectron corresponds to a direct knock out when the whole of the photon energy and angular momentum is absorbed by the fast photoelectron.

In TPDI, because the target atom interacts with the field twice, the shake-off electron can be ejected in a p wave after firstly being promoted from the ground $1s$ state to an excited np state. In this scenario, the main contribution to the angular distribution of the slow electron comes from the $l_1 = l_2 = 1$ term which leads, in the dominant quadrupole channel, to $\beta_2 = 1$ and $\beta_4 = 0$. This is indeed close to the calculated value of β_2 and explains much smaller values of β_4. By way of the exchange symmetry, one can argue that the same angular terms would be dominant for the fast electron which explains a rather weak energy dependence of β parameters. A non-zero value of β_4 indicates that the slow electron can also emerge in a d state as a result of two repeated knock out processes.

3.5. Recoil ion momentum distribution

By integrating the squared amplitude (9) over the spherical angle $d\Omega_{\boldsymbol{k}}$ we get the DDCS $d^2\sigma/(d\Omega_p dE_p)$ which is given by the expression equivalent to Eq. (10). The angular anisotropy parameters β_2, β_4 and the SDCS $d\sigma/dE_p$ entering this expression are shown in Figure 5 in comparison with the corresponding parameters for SDCS.

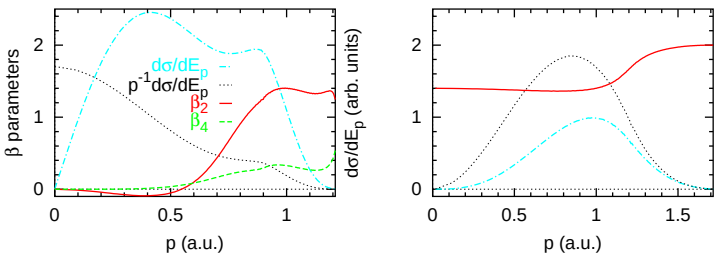

Figure 5. (Color online) Angular anisotropy β parameters and energy distribution $d\sigma/dE_p$ of the recoil ion for single-photon (right) and two-photon (left) double ionization of He at the excess energies of 11 and 20 eV, respectively.

Again, as in Figure 4, there is a qualitative difference between the TPDI and SPDI cases. In the two-photon case, the β parameters change from nearly zero to large positive values as p varies from 0 to $p_{\max}$. This is to be compared with the large and positive β_2 parameter which varies very little in SPDI. The energy distribution $d\sigma/dE_p$ is zero both for $p = 0$ and $p = p_{\max}$ ($k = 0$) due to the kinematic factor kp. However, the function $p^{-1}d\sigma/dE_p$ is large at $p = 0$ and decays monotonously towards $p_{\max}$ in TPDI but has a broad maximum at about $\simeq p_{\max}/2$ in SPDI.

This different behavior of double ionization amplitudes in single- and two-photon case has a profound implication when the recoil ion momentum distribution is measured experimentally

which can be seen seen in Figure 6. For SPDI, this momentum distribution peaks at $\simeq p_{\max}/2$ where β_2 is large and positive resulting in a broad dipole structure aligned along the polarization axis of light as is indeed the case for various excess energies ranging from 1 to 100 eV [22]. On the contrary, in the TPDI case, the intensity of the momentum distribution is largest near the origin where the β parameters are close to zero. Hence, there is very little anisotropy seen in the recoil ion momentum distribution except for large momenta where the experimental signal is fairly weak.

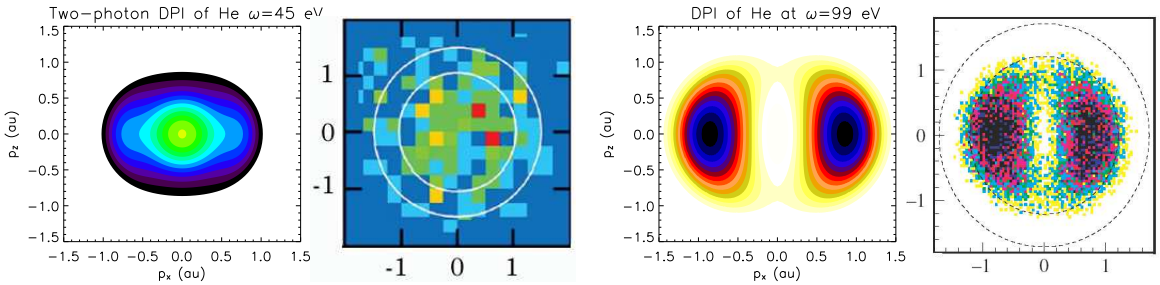

Figure 6. (Color online) Recoil ion momentum distribution $d\sigma/(dp_x dp_z)$ in two-photon (first and second left) and single-photon (first and second right) double ionization. Experimental data are from Refs. [23] and [21] for TPDI of Ne at 38.8 eV and SPDI of He at 99 eV, respectively.

References

[1] Bray I, Fursa D V, Kheifets A S and Stelbovics A T 2002 *J. Phys. B* **35** R117–R146
[2] Ivanov I A and Kheifets A S 2005 *J. Phys. B* **38** 2245
[3] Kheifets A S 2004 *Phys. Rev. A* **69** 032712
[4] Ivanov I A and Kheifets A S 2007 *Phys. Rev. A* **75** 033411
[5] Tang X and Bachau H 1993 *J. Phys. B* **26** 75–83
[6] Dyall K G, Grant I P, Johnson C T, Parpia F A and Plummer E P 1989 *J. Comp. Phys.* **55** 425–456
[7] Bray I and Stelbovics A T 1995 *Adv. Atom. Mol. Phys.* **35** 209–254
[8] Cormier E and Lambropoulos P 1995 *J. Phys. B* **28** 5043
[9] Nikolopoulos L A A and Lambropoulos P 2001 *J. Phys. B* **34** 545
[10] Feng L and van der Hart H W 2003 *J. Phys. B* **36** L1–L7
[11] Piraux B, Bauer J, Laulan S and Bachau H 2003 *Eur. Phys. J. D* **26** 7
[12] Hu S X, Colgan J and Collins L A 2005 *J. Phys. B* **38** L35
[13] Martín F 2007 *ECAMP IX: Satellite Symposium on Multiphoton multiple ionisation of atoms, molecules and clusters* Crete, Greece
[14] Kheifets A S and Ivanov I A 2006 *J. Phys. B* **39** 1731–1742
[15] Lambropoulos P, Nikolopoulos L A A and Makris M G 2005 *Phys. Rev. A* **72** 013410 (pages 4)
[16] Colgan J and Pindzola M S 2002 *Phys. Rev. Lett.* **88** 173002
[17] Huetz A, Selles P, Waymel D and Mazeau J 1991 *J. Phys. B* **24** 1917–1933
[18] Malegat L, Selles P and Huetz A 1997 *J. Phys. B* **30** 251–261
[19] Istomin Y A *et al.* 2006 *Phys. Rev. Lett.* **97** 123002
[20] Kheifets A S, Ivanov I A and Bray I 2007 *Phys. Rev. A* **75** 024702
[21] Bräuning H *et al.* 1997 *J. Phys. B* **30** L649–L655
[22] Knapp A *et al.* 2002 *J. Phys. B* **35** L521–L526
[23] Moshammer R *et al.* 2007 *Phys. Rev. Lett.* **98** 203001